I.FAST

Innovation Fostering in Accelerator Science and Technology

Horizon 2020 Research Infrastructures GA n° 101004730

DELIVERABLE REPORT

Electron acceleration experiments with new targets

DELIVERABLE: D6.3

Document identifier:	IFAST-D6.3
Due date of deliverable:	End of Month 24 (April 2023)
Report release date:	30/04/2023
Work package:	WP6: Novel particle accelerators concepts and technologies
Lead beneficiary:	CNRS
Document status:	Final

ABSTRACT

Laser-Plasma Accelerators (LPA) exploit electric fields exceeding 100 GV/m to produce ultrashort electron bunches. These unique features open up new prospects for ultrafast physics and the development of compact accelerators. Yet, LPAs suffer from inferior beam quality and stability. One of the reasons for these weaknesses is poor control of the target properties. Task 6.3 aims at developing and testing targets of superior quality for extending the beam energy and improving its reliability. Here we report on experiments performed with the new targets, showing excellent performance.

I.FAST Consortium, 2023

For more information on IFAST, its partners and contributors please see https://ifast-project.eu/

This project has received funding from the European Union's Horizon 2020 Research and Innovation programme under Grant Agreement No 101004730. IFAST began in May 2021 and will run for 4 years.

Delivery Slip

	Name	**Partner**	**Date**
Authored by	C. Thaury	CNRS	30/04/2023
Reviewed by	M. Vretenar [on behalf of Steering Committee]	CERN	30/04/2023
Approved by	Steering Committee		30/04/2023

TABLE OF CONTENTS

Executive summary

The general objective of work package 6.3 is to develop multi-scale innovative targets for laser-plasma accelerators and demonstrate improved electron beam features with the new targets. Deliverable D6.3 reports on the laser-plasma acceleration experiments carried out, using the targets developed and characterized in Year 1 (see MS23). We have developed two different classes of targets: ultrashort targets compatible with high repetition rate laser-plasma accelerators (LPA) and long targets for producing very high energy electron beams at a lower repetition rate.

On our kHz LPA facility, we worked on a new design of a micro-scale gas nozzle. The nozzles are made from sapphire, which provides high thermal conductivity and transparency to laser light. They were manufactured using the FLICE technique (Femtosecond Laser Irradiation and Chemical Etching) at FTMC. This technique allows for high-precision microscale machining and makes it possible to produce asymmetric shocked supersonic jets on a 100-micrometer scale. This geometry is ideal for density transition injection, which allows for stabilizing electron injection into the accelerating wakefield. Experiments were performed with these nozzles, leading to the generation of stable 3-4 MeV beams for 5 hours at a 1 kHz repetition rate, totaling millions of shots. We found the jets to be much more resistant to damage than metal nozzles, and the shock helped a lot in stabilizing the injection. We also focused on the effect of the laser carrier-envelope phase (CEP). The effect of the CEP is usually overlooked in laser-plasma acceleration but it was predicted to become noticeable for few-cycle laser pulses. We performed a series of unique experiments demonstrating the clear effects of the CEP on the electron beam-pointing. This was possible thanks to the high stability of our LPA.

At high energies, we developed a plasma waveguide target. The technique is based on the use of an innovative optic, the axiparabola, to focus a laser prepulse over a long line in a gas jet. This prepulse creates a plasma column that expands in a plasma channel. The latter is then used to guide the intense laser pulse which drives the accelerator. The waveguide was successfully used at LOA to keep focused an intense laser over a 15 mm gas jet and increase the energy gain of the accelerator from 300 MeV to 1.1 GeV. The injection was triggered using the density transition technique, by placing a sharp blade in the gas flow. We then developed an 8 cm long target, using the same technique, and managed to produce a 2.4 GeV electron beam with a narrow energy spread, at the Apollon laser facility.

1 Introduction

Laser-Plasma Accelerators (LPA) exploit electric fields exceeding 100 GV/m to produce ultrashort electron bunches, at energies ranging from a few MeV, to several GeV. These unique features open up new prospects for ultrafast physics and the development of compact accelerators. Yet, LPAs suffer from inferior beam quality and stability. One of the reasons for these weaknesses is poor control of the target properties.

The ideal gas targets should meet several criteria. First, it should reliably produce a homogeneous gas cloud with a well-controlled density. Second, it should be able to generate sharp density gradients, with typical scales of about 10 µm or smaller. These sharp density gradients allow the control of electron injection into the accelerating field, leading to higher-quality electron beams with low relative energy spreads and higher stability. Lastly, the generation of high-energy electrons (> 1 GeV) requires long targets (with lengths that can reach several cm or tens of cm, depending on the laser energy) and, ideally, a transverse structure able to guide the intense laser over this distance.

The elaboration of such targets is particularly challenging as these requirements are partly contradictory. While long and homogeneous centimeter-scale plasmas are required for accelerating electrons to high energies, precise tailoring at the 10 µm level is critically important for controlling the injection. Therefore, while the need for a reliable and homogeneous gas cloud favors the use of a gas cell, it makes it difficult to produce sharp gradients. Conversely, gas jets can generate sharp gradients, using supersonic gas jets or hydrodynamic shocks, but at the price of lower reliability. They are also less suitable for achieving long targets, and their length has until now been limited to about 1 cm.

The main objective of WP 6.3 is to overcome these limits by relying on the best of existing technologies. A hybrid 3D laser machining method (FLICE: Femtosecond Laser Irradiation and Chemical Etching) developed by Vidmantas Tomkus' group at FTMC is used to fabricate gas nozzles with apertures as small as 50 um and high surface quality [1]. This technique provides better plasma density control at the sub-100 micron scale, where conventional machining techniques such as electro-erosion begin to fail. In addition, the FLICE technique makes it possible to manufacture dielectric gas jets, unlike the metal jets usually used in LPA. Dielectric nozzles have a higher damage threshold than metal nozzles, which leads to higher resistance to laser radiation and, therefore, better reliability.

These innovative nozzles can produce density gradients on the microscopic scale, yet, they are not suitable for generating gas clouds several centimeters long and, therefore, for accelerating beams of several GeV. Until 2021, the most effective target for obtaining electron beams in the GeV range was the capillary discharge [2]. But this device suffers from substantial drawbacks, linked to the fact that the plasma is encapsulated in a capillary. In particular, it is challenging to shape the plasma and avoid damaging the capillary. Thus, this target does not reliably produce quality beams. To overcome these limitations, we have developed an entirely optical technique to produce long plasma waveguide targets [3].

Microscales and long targets were developed and characterized during year 1 of the project, as reported in MS23. We present here the experiments carried out with these innovative targets that led to a significant improvement in the reliability of the accelerator and the quality of the beam, both in the kHz regime and at very high energy.

2 Ultrashort nozzles for kHz repetition rate accelerators.

2.1 MICRO-SCALE SHOCK NOZZLES

High-repetition rate laser-plasma accelerators with an energy of only a few milli-joules per pulse require targets with a typical length of about 200 μm. Several targets have been tested, with either symmetrical or asymmetrical designs [4]. Here, we present the results obtained with the asymmetrical nozzle which gave the best results. The nozzles were made from sapphire using the FLICE technique. It consists of a 100 μm throat and 300 μm exit diameter "De Laval" nozzle to which a 100 μm long flat section has been added at the end of one of its sides. The nozzle design and characterization are presented in MS23. The peak electron density at the nozzle exit was 9.7×10^{19} cm^{-3} and the density after the shock was 7.3×10^{19} cm^{-3}, corresponding to a 25% density drop with a transition width of 15 μm. The experiment was conducted using the Salle Noire laser system at LOA which provides 3.8 mJ, 4 fs beams at a 1 kilohertz repetition rate.
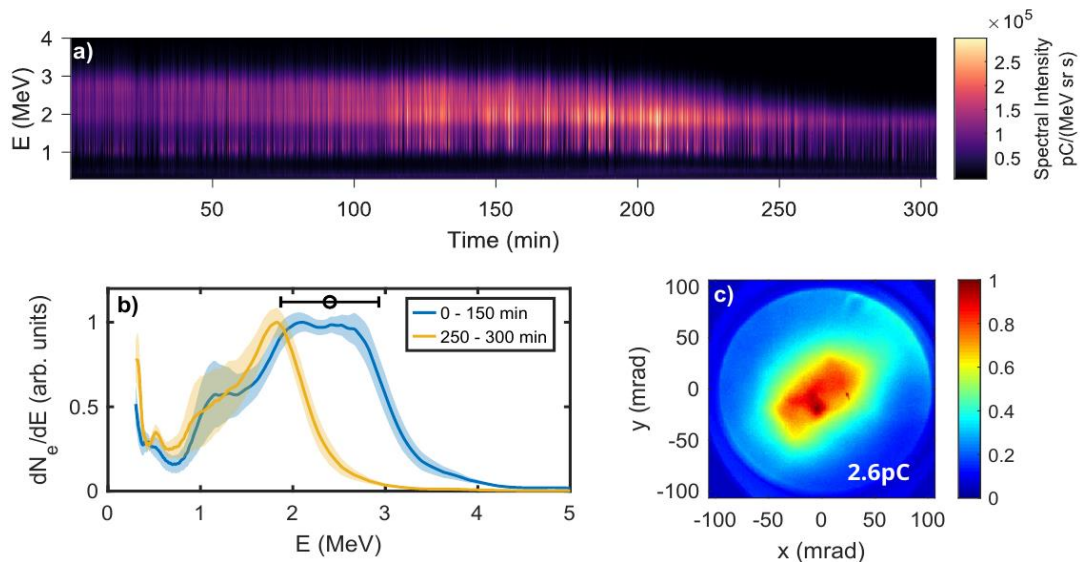

Fig. 1 a) Electron spectra measured continuously for 306 min. Each spectrum is averaged over 100 shots. b) Electron spectra averaged over 0-150 min (blue) and 250-300 min (orange), and their standard deviations (shaded area); the black error bar represents the spectrometer resolution at 2.4 MeV. c) Electron beam measured just before the start of the 5h spectrum monitoring. The total charge per shot is 2.6 pC ± 0.6 pC (std). The beam divergence is approximately 80 mrad FWHM.

Statistics were performed from 20 acquisitions, each consisting of an accumulation of over 10 shots, thus accounting for 200 shots in total. This initial measurement yielded a mean charge of 2.6 pC per shot with a 0.6 pC standard deviation, and a beam divergence of 80 ×75 mrad ± 8 × 9 mrad FWHM(see Fig.1c). Electron beam-pointing stability is 17 ×11 mrad RMS. This regime was obtained by setting the focal point of the laser at the position of the shock-front, strongly suggesting that the injection occurs indeed at the density transition. **The electron spectrum was then monitored during 5 hours of complete hands-off operation of the kilohertz laser-plasma accelerator**, i.e. with no other intervention than the automatic beam-pointing stabilization feedback loops in the laser chain. The results of this measurement are displayed in Fig.1a [5]. **Beams with peaked spectra and a large majority of electrons with energy exceeding 1 MeV were reliably produced throughout the**

whole 306 min of monitoring. Moreover, during the first 150 min, the spectrum remained very stable, with a peak energy of 2.5 MeV. After that, the high-energy part noticeably eroded with time, lowering the peak energy to 1.9 MeV. A comparison of the spectra during the first 150 min and the last 50 min is represented in Fig. 1b. To complete these data and assess more thoroughly the question of stability, we plot the temporal evolution of the total charge per solid angle $dQ/d\Omega$ collected through the pinhole of the spectrometer (Fig. 2a), the mean energy of the electrons $\langle E\rangle$ (Fig. 2b), as well as the relative laser energy at different points of the laser chain (Fig. 2c). All curves are averaged over a 1 min moving window. The data show an increase in $dQ/d\Omega$ (Fig. 2a) during the first 130 min. This is likely due to a small angular drift of the electron beam on a long time scale, resulting in a higher electron signal through the electron spectrometer pinhole. Therefore, only the short-term variation of the charge can be estimated with certainty from this measurement, giving the typical fluctuation of about 50 pC/(sr shot) corresponding to 20% RMS.
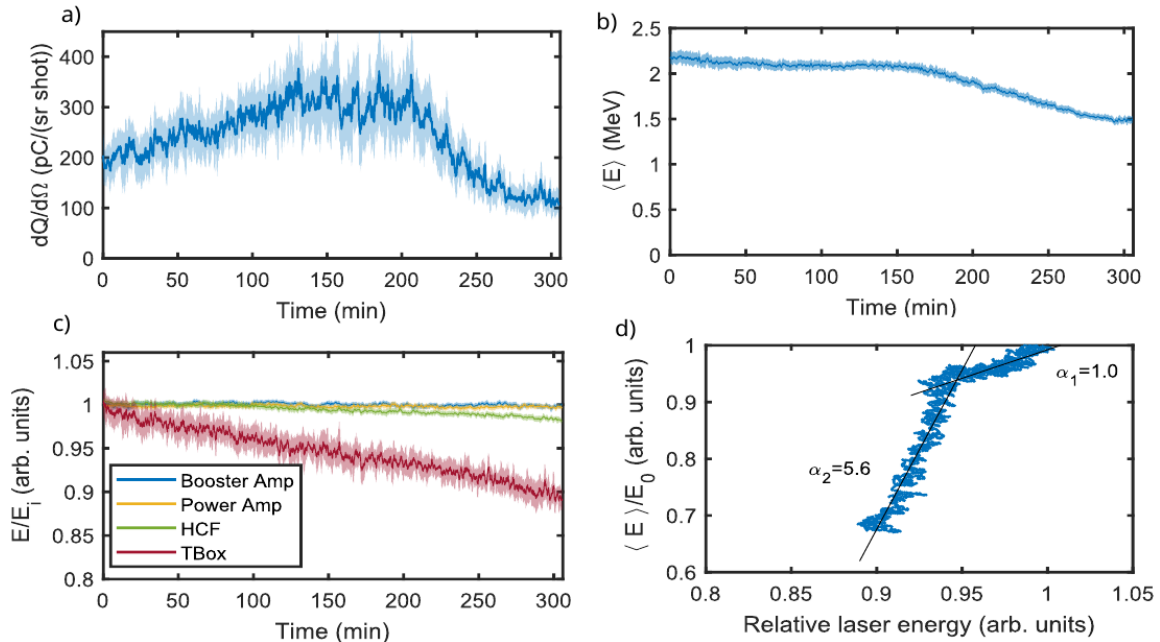

Fig. 2 a) Total charge per solid angle collected through the electron spectrometer pinhole. b) Mean electron beam energy versus time. c) Monitoring of the laser energy at four points in the laser chain. Each curve in this figure is averaged over a one-minute moving window and shaded areas represent the corresponding standard deviation. d) Correlation between the electron mean energy and the relative laser energy right before the off-axis focusing parabola, and linear fits of the two different parts of the curve, with slopes α1 and α2.

Figure 2b confirms the observations made previously regarding the stability of the spectrum, and indeed, shows that the mean energy of the electrons is quite stable at $\langle E\rangle \simeq 2.1$ MeV during the first 150 min of monitoring, with short-term RMS variations of only 2-4% (shaded area in Fig. 4.9b). The decrease of the mean beam energy to $\langle E\rangle \simeq 1.5$ MeV toward the end of the run can also be observed. Note that during the run, the laser system was extremely stable, see Fig. 2c, except for the energy measured using the turning box diagnostic (red curve in Fig. 2c), which is the last measurement point before the focusing parabola and is, therefore, the most representative of the evolution of the laser energy on target. The energy measured at this point decreased steadily during the experiment and reached an 11% relative loss after 306 min. This progressive energy loss was due to the slow damage of a few chirped mirrors at the end of the compressor. Interestingly, the evolution of the electron energy can be correlated to the evolution of the laser energy at this last measurement

point. To display these correlations, Fig. 2d shows the normalized mean energy of the electrons plotted against the laser relative energy. Two different correlation regimes are distinguishable: (i) the first 5% of laser energy loss leads to a ∼ 5% energy loss of the electrons suggesting a linear correlation. We then observe a threshold effect, (ii) as the next 5% drop of laser energy correlates with a ∼30% electron mean energy loss. Assuming a linear dependence in both regimes, the two parts of the correlation plot are linearly fitted, yielding a slope α1 = 1.0 in the first five percents of energy loss, and a slope α2 = 5.6 in the following five percents. **This highlights the importance of laser energy stability**: in our case, energy variations larger than 5% can cause significant modifications of the electron spectrum due to what seems like a threshold effect. Nevertheless, decent stability of the electron beam was achieved over the 300 min of continuous operation, with the first 150 min period displaying remarkable stability correlated to the highest laser performance.

To determine the repeatability of the electron beam and to assess the sensitivity of the accelerator to small day-to-day variations of the laser parameters, the measurements were repeated on three different days, each separated by about a week. The same actual nozzle was used for the three experimental runs and kept its integrity over time. Table 1 summarizes experimental conditions for each day, as well as the charge and mean electron energy corresponding to the electron spectra displayed in Fig. 3. **These results show that the downward gradient injection method with one-sided shock nozzles increased significantly the reliability of the accelerator.** Indeed, electron beams with similar charge and 2-3 MeV peaked spectrum were easily obtained even though the experimental parameters varied slightly from day to day. In particular, we see that experiments from day 2 and day 3, performed at the same plasma density, yield very similar electron spectra. Such a level of reproducibility is decisive for the reliable use of the accelerator for applications. **Moreover, the fused-silica nozzles showed great resilience to damage, as the one used for this experiment provided reliable and reproducible results even after using it for about 50×10^6 shots.**

	Day 1	Day 2	Day 3
I (W.cm^{-2})	1.8×10^{18}	2.0×10^{18}	1.6×10^{18}
$n_{e,peak}$ (cm^{-3})	8.8×10^{19}	9.7×10^{19}	9.7×10^{19}
Q (pC/shot)	1.6±0.2	2.6±0.6	1.4±0.2
div. fwhm (mrad)	42±10	77±7	57±11
$\langle E \rangle$ (MeV)	2.29±0.13	2.11±0.06	2.19±0.04

Table 1 – Various experimental parameters and electron beam performance showing slight variations from day to day but overall fair reproducibility of the experiment. The values after the ± sign are RMS deviation.
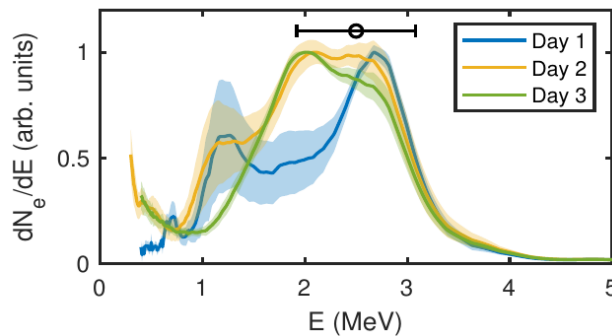
Fig. 3 Electron spectra obtained on three different days with the same one-sided shock nozzle. Spectra are the results of averaging over 2000 shots for day 1 and day 2, and 5000 shots for day 3. Day 1 and day 2 are 7 days apart, day 2 and day 3 are 6 days apart.

2.2 CONTROL OF THE LASER CARRIER-ENVELOP-PHASE

Thanks to the high acceleration stability obtained with the newly developed shock nozzles, we were able to perform a study on the effects of the carrier-envelop phase of the laser. This effect is usually neglected in laser-plasma accelerators, but it was predicted that it would become noticeable for laser pulses of a few cycles. A supersonic nitrogen gas jet, with a 60 μm throat and 180 μm exit diameter is used. Supersonic gas jets were chosen over one-sided shock jets because it was observed in simulations that gradient injection leads to significantly reduced effects of the carrier-envelope phase on the accelerated beam [6]. During the experiments, the CEP was varied by increments of π/4, and the electron beam parameters were measured for each CEP value. We repeated the CEP loop two or three times to ensure that the variations were repeatable with CEP and not associated with slow drifts of the accelerator. Figure 4 presents data from a CEP scan between 0 and 2π repeated on three loops, at a plasma density of $n_e = 1.4 \times 10^{20}$ cm^{-3}. The panels a) and b) show a clear dependence of the electron beam-pointing in the polarization plane to the CEP, as it repeatedly oscillates during the three loops, with a significant amplitude of about 15 mrad (∼ 30% of the beam divergence which is 50 mrad). In the perpendicular direction, the pointing does not vary with CEP, which is expected as single-cycle pulses induce no asymmetry in this plane. These pointing fluctuations can be an important source of instability of the electron beam. Indeed, we can estimate the maximum sensitivity of the beam-pointing to the CEP by measuring the maximum slope of the pointing oscillations: dθ y /dφ = 20 mrad/rad, meaning **it would be necessary to stabilize the CEP to 50 mrad RMS to keep the pointing variations under 1 mrad (not considering other sources of pointing jitter). This highlights the importance of CEP-control in the perspective of the development of a stable laser-wakefield accelerator driven by (near)-single cycle pulses [7].**
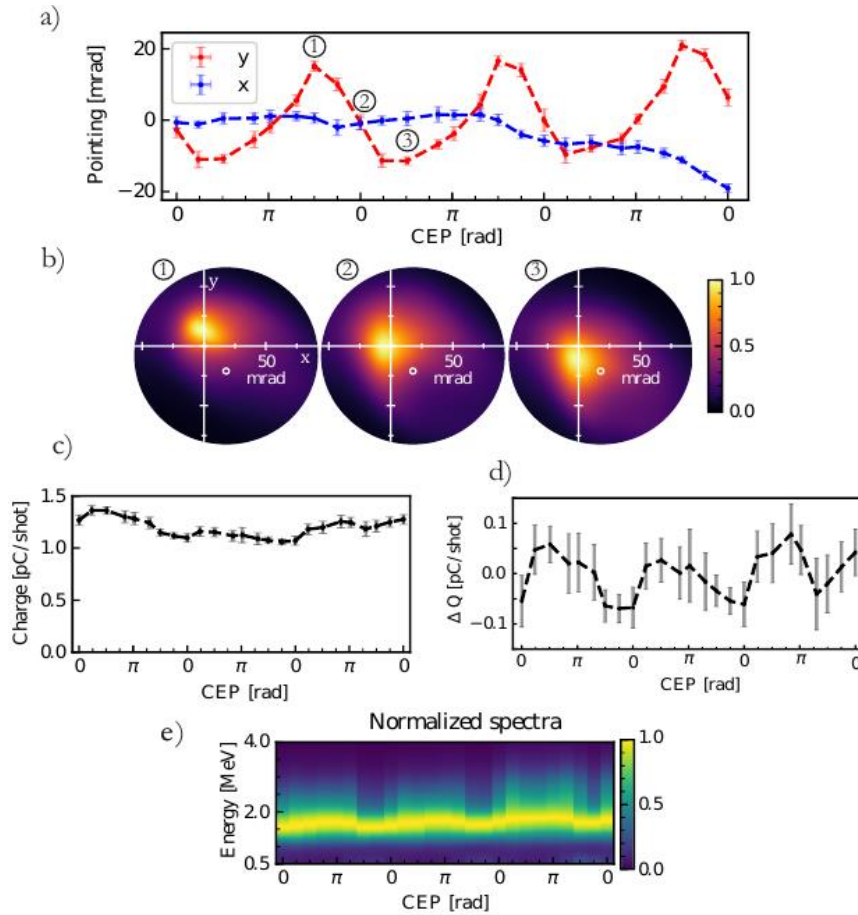
Fig. 4 Experimental results obtained at ne = 1.4 × 1020 cm−3 when varying the CEP. a) Electron beam-pointing in the laser polarization direction (y,red) and in the perpendicular direction (x,blue). b) Electron beam profiles acquired by accumulating 200 consecutive shots, for three different laser CEP corresponding to (1) high, (2) central, (3) low beam-pointing. The small white circle corresponds to the position of the sampling pinhole of the spectrometer. c) Electron beam charge as a function of CEP. d) Charge variations as a function of CEP. The slow non-periodic fluctuations are removed by performing a moving average on 2π. e) Normalized electron spectra as a function of CEP. Pointing, charge, and spectra data are averaged on 20 measurements of 200 consecutive shots (4000 shots per point in total). The error bars are obtained by estimating the standard deviation on these 20 measurements.

The accelerated charge is shown in Fig. 4c and is in the picocoulomb range. By performing a moving average on 2π to remove the non-periodic slow variations, we bring out a slight charge modulation of the order of 8% depending on the CEP (see Fig. 4d), but this behavior is not as clear as the one observed on beam-pointing because it is dominated by charge variation uncorrelated to CEP. The electron mean energy is around 1.9 MeV, and the normalized electron spectra as a function of the laser CEP are plotted in Fig.4e. They show that the measured energy of the electron oscillates moderately with CEP, with variations of 5% of the mean energy. But additional measurements showed that this effect is mainly caused by a difference in the sampling of the beam in the spectrometer due to the beam-pointing changing with CEP. As can be seen in Fig. 4b, the pinhole of the spectrometer represented by the small white circle samples different parts of the beam depending on the CEP. As the energy distribution is not spatially uniform, this lead to fluctuations in the measured energy even if the global beam energy remains constant.

The fact that the charge is strongly impacted, but not the energy of the electrons indicates that the carrier-envelope phase mainly plays a role in injection, and not really in the subsequent acceleration

mechanism. Numerical simulations and additional experiments allowed us to identify two main sources for these effects:

- The transverse oscillation of the asymmetry of the wakefield associated with near-single-cycle pulses can trigger periodic off-axis injection of bunches whose final pointing depends on the value of the asymmetry at the moment of injection. We have observed experimentally that this effect leads principally to a variation of the electron beam-pointing in the polarization direction, but also to significant change in the injected charge in some cases. These observations demonstrate the breakdown of the ponderomotive approximation for near-single-cycle pulses and show the importance of considering the actual shape of the electric field in this case.

- Ionization injection leads to the injection of electrons from the extrema of the laser electric field and is therefore sensitive to the CEP. We have been able to observe preliminary experimental results of CEP effects on ionization injection using a He/Ar mixture indicating an energy dependence on the direction of the beam in the polarization plane. If a more thorough control was achieved, the CEP of a single-cycle pulse could be used to finely control the position of injection of electrons, for example in an accelerator driven by a particle beam.

This work provides an experimental and numerical study of both regimes of CEP effects, but additional questions remain to address. It has been observed numerically in [6] that gradient injection reduces the impact of the carrier-envelope phase on injection, this is interesting in the context of minimizing the negative effects associated with the off-axis injection due to the transverse oscillation of the bubble, and would require experimental demonstration. Similarly, it has been observed that using a laser with circular polarization reduces the final beam divergence by minimizing the transverse oscillations associated with CEP. Our setup with stabilized and controlled CEP would allow us to quantify more precisely this effect, but achieving a clean circular polarization remains a challenge.

3 Long nozzles for GeV accelerators.

3.1 FIRST EXPERIMENTS AT 1 GEV

Along with increasing the repetition rate of the accelerator, one of the main challenges of laser-plasma acceleration is to produce beams that combine high energy and high quality. Different solutions have been developed to answer this challenge.

(i) The longer the relativistic laser-plasma interaction, the higher the electron energy is. However, the distance where the laser intensity is at maximum is limited by diffraction to the Rayleigh length. In laser-plasma interaction, the physical process of auto-focusing increases the acceleration length to a few Rayleigh lengths under precise physical conditions. Nevertheless, this acceleration length is always limited in practice to typically a couple of mm because of the decrease of the laser power during the interaction. To increase the accelerating length to the cm-scale, instead of using a gas jet, a new type of gas target has been developed: the capillary discharge. The idea is that the discharge in the capillary ionizes the gas a few ns before the laser pulse to create a plasma channel. This channel then acts as an optical fiber that guides the high-intensity laser pulse over long distances. Thanks to

this technique, 1 GeV electron beams were obtained with a 3.3 cm propagation of a 40 TW laser beam [2] and up to 8 GeV with a 20 cm propagation [8]. While this technique enables to obtain very high electron energies, it has several drawbacks. First, the capillary makes it challenging to perform shaping on the gas profile to optimize the interaction parameters. Second, the thin diameter capillary can be damaged by the high-energy laser, especially at the low densities required to produce GeV-class electron beams.

(ii) To obtain a relative energy spread of the order or below the percent, several strategies have been proposed. The key idea is to constrain the trapping of the electrons at the very beginning of the interaction and to prevent the trapping in the following propagation. This way, all the electrons experience the same accelerating length and are accelerated to the same energy. A simple strategy consists in shaping longitudinaly the density profile of the gas at the beginning of the interaction to have a transition from a high density to a lower one. The increase of the size of the plasma bubble at the density transition slows down the wakefield which enables to localize the electron trapping in this region. In practice, the density shape can be efficiently obtained by generating a hydrodynamic shock in a gas jet. For instance, a blade inserted at the output of a gas jet, just below the laser axis, creates a shock of a few 10 µm scale at the entrance of the gas target. A long region of constant density can then be used for acceleration.

We have developed a novel strategy to solve at once the two scientific issues listed in (i) and (ii). The principle is to create a plasma guide optically with a prepulse that ionizes the gas a few ns before the main pulse. After the ionization by the prepulse, the plasma density expands toward the radial direction and thus forms a hollow channel around the optical axis, similar to a capillary discharge. This plasma channel acts as an optical fiber that guides the main laser pulse over a long distance. This guiding technique has three main advantages.

    1- First, as the guide is optically created with a second laser pulse, the coupling of the main beam into the plasma guide is directly controlled by the pointing of both laser beams and can have therefore high stability.

    2- Second, as the guide is not created with the technological development of a complex target design, a simple gas jet can be used therefore enabling to shape the density profile of the gas.

    3- Third, the technique works for arbitrary density and the waveguide is immune to laser damage. It is therefore usable for arbitrarily high laser power and at high repetition rates.

A major difficulty to overcome for generating such a plasma guide is to focus the prepulse beam along a line of the scale length of the desired guide along the optical axis. To fulfill this requirement, we proposed to use a specific optic named axiparabola. It is an aspheric mirror that reflects a collimated beam into an extended focal line by focusing rays at different focal planes depending on their radial coordinate on the mirror [9]. This enables to focus a laser beam in a long focal line of a few cm, within a tiny radial dimension of only a few-10 µm [3].

we have performed at LOA the first LPA experiment in such a waveguide [11]. The experimental scheme is illustrated in Fig. 5a. A first beam P2, is focused by an axiparabola into a long gas jet of 1.5 cm. After 2 ns, the main beam P1 is focused at the entrance of this gas jet along the same axis (thanks to a hole at the center of the axiparabola). It propagates in the plasma guide and accelerates

electrons by LPA. After the interaction, the electron energy is measured with an electron spectrometer (magnet + phosphor screen), panels (c), and the laser beam is imaged at the jet output by a high flux focal spot diagnostic, panels (d). In addition, a probe beam (P3) images the plasma guide from its side with the help of a wavefront sensor to retrieve the electron density profile, panels (b).
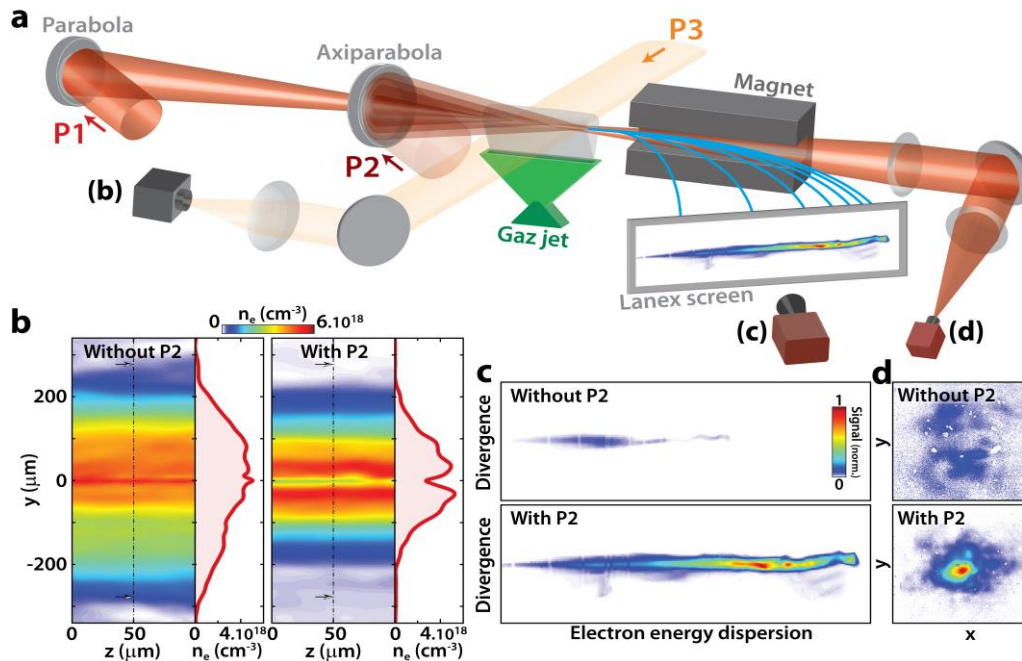

Fig. 5 Electron acceleration in a laser-plasma waveguide. The generation beam, P2, is focused in the target, 2 ns before the main beam P1, by an f/4 axiparabola. It generates a plasma waveguide (shown in b) which can keep P1 focused over long distances. The main beam, P1, is focused by an f/18 spherical mirror. It accelerates electron bunches whose energy is then analyzed with a spectrometer consisting of a dipole magnet, a LANEX scintillating screen, and a 16 bits camera (e). It is eventually attenuated to image its focal spot after interaction (f).

As can be observed in Fig. 5b, when the pre-pulse ionizes the gas a few ns before the main pulse, a plasma guide (with a hollow at its core) is created. Thanks to this channel, the laser beam is guided over 15 mm and hence still focused at the output of the gas jet (panels d), and, most of all, the charge and the maximum energy of the electron bunch are strikingly increased. Figure 6 shows the corresponding energy spectra angularly resolved of the electron beam for four consecutive laser shots (panel a), and the angularly-integrated energy spectra for 50 consecutive shots which are compared with typical spectra obtained without the plasma guide (without creation beam). As can be observed here, not only the charge and the energy of the beam are increased, but this improvement occurs at each laser shot, demonstrating the remarkable gain in the beam quality enabled by this technique. The total charge above 350 MeV exceeds 50 pC, meaning that about 2.2% of the laser energy in the laser focal spot was transferred to electrons above 350 MeV.
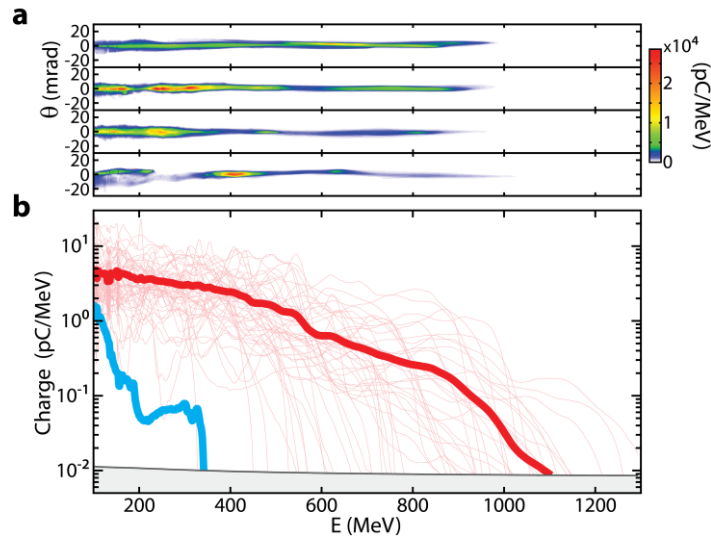
Fig. 6 Electron spectra with guiding. (a) Four angularly resolved consecutive shots. (b) Fifty consecutive shots (light red), average spectrum (thick red line), and best shit without guiding (blue line).

This all-optical scheme to create the plasma waveguide allows the use of a gas jet as a target, which provides easy access to the gas density and thus enables to shape its profile along the laser propagation axis. To control the injection and produce electron beams with a peaked energy spectrum, we have associated this optically controlled plasma waveguide with the shaping of the gas density profile with a hydrodynamic shock. Figure 7 shows a typical energy spectrum obtained in this experiment. **The accelerated beam consists of a narrow peak centered at 1.15 GeV, with a high peak charge and remarkable shot-to-shot stability. The energy spread was measured to be below 4% FWHM for the best shots, with a conversion efficiency from the laser to the beam of about 1%**. This conversion efficiency can reach 6% for the most loaded beams which however have a larger energy spread. To the best of our knowledge, this is the first time that GeV-range, stable monoenergetic beam has been obtained, using LPA.
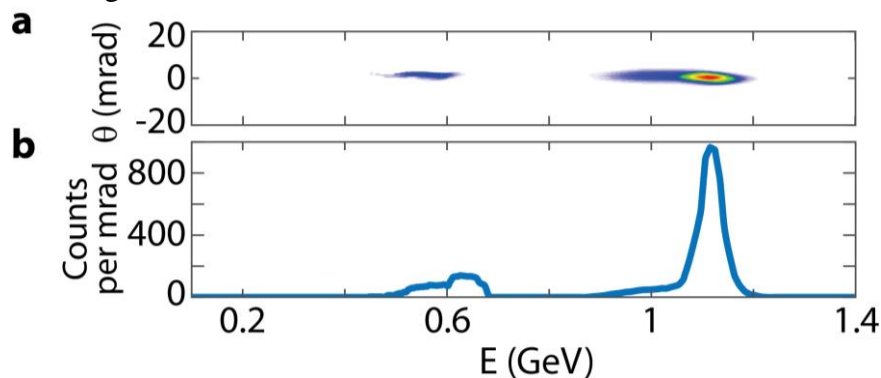

Fig. 7 Typical electron beam obtained by injecting an electron beam in a laser-plasma waveguide, using the density-transition injection technique.

3.2 MULTI-GEV ACCELERATION

Following the guiding experiments at LOA, we have adapted the setup to perform the same experiment, at higher energy, on the PW Apollon installation. It implied the development of several

bricks that have been tested for the first time during the experiment including a massive, 1.3 m-long, 10 GeV spectrometer, and an on-axis axiparabola at f/20 producing an 8 cm long focal line (used to generate a several-cm-long plasma waveguide). As the facility is not currently designed for multi-beam experiments, one of the main challenges was to split the laser beam into 3 beams with adapted energies and delays. This implied the development of several optical systems for, attenuating the beams, controlling their delays, and changing their diameters. A picture of the experimental setup is shown in Fig. 8.

Fig. 8 View of the experimental chamber

The installation of these devices and the setting up of all the diagnostics consumed most of the beam time. We had only a few days left for the actual experiment. Nevertheless, **we were able to assess the good guiding of the laser and observed a significant increase of the electron beam energy from 1.2 to 2.3 GeV when using the guide**, as illustrated in Fig. 9. Yet, because of the lack of stability of the laser pointing, the relatively low number of shots per day, the impossibility to increase the gas pressure at will (because of pumping issues), and all the time spent on solving technical problems, we were not able to achieve an actual optimization and obtain statistics.
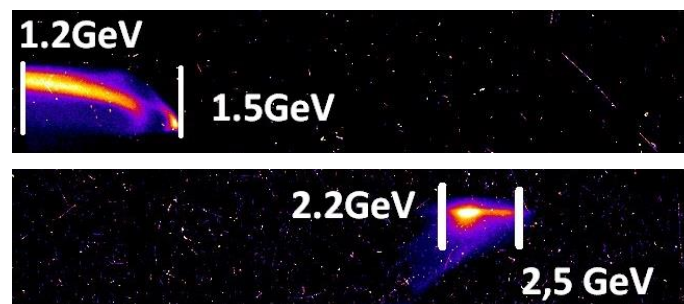

Fig. 9 Angularly resolved electron spectra without (top) or with (bottom) the waveguide. Laser focus and gas density are optimized in both cases. The two spectra correspond to the highest energies measured in both conditions during one day.

Even if the energy is lower than that initially targeted (4 GeV were aimed at). These results constitute a success in the sense that it is the first time that an electron beam is injected in a controlled manner and then accelerated in a plasma waveguide, at this energy level. All the concepts and techniques involved are validated. It now remains to optimize the parameters to increase the energy and make the source more reliable.

4 Conclusion and relation to other WP6 tasks

The nozzles we have developed have allowed us to significantly improve the performance of our laser-plasma accelerators, both at low-energy high-repetition-rate and at very high energy. At a high repetition rate, we have taken the experiment to a new stage of operation by stabilizing and rationalizing the injection process by using newly designed one-sided shock nozzles. We have demonstrated a continuous hands-off operation of our accelerator, accumulating a record of more than 18 million consecutive shots, and good repeatability of the electron beam from one day to another. Secondly, we observed and controlled the effects of the carrier-envelope phase of the laser pulse on the electron beam parameters, mainly through the observation of variation in the electron beam-pointing when changing the CEP, but also significant charge fluctuations of up to 30% in some cases. We attributed these effects to the transverse oscillations of the wakefield in the polarization direction associated with the slippage of the CEP.

At higher laser energies, we have developed an efficient plasma waveguide for LPA. The waveguide is generated with an all-optical method and coupled with a controlled injection technique to produce high-quality, multi-GeV electron beams. It was first demonstrated using a 50 TW-class laser to produce 1.1 GeV beams with an energy spread below 4%, and then on the PW Apollon laser facility to generate quasi-monoenergetic beams with a peak energy of 2.3 GeV. To our knowledge, this is the first time that good-quality beams have been repeatedly produced at this energy level.

The relations of this work with the other tasks are numerous. First, we have demonstrated, using new generation targets, that LPA can be operated reliably at a repetition rate of 1 kHz, which is an important step for the development of high-average current laser-plasma accelerators. We have also highlighted the importance of CEP-control in the development of a stable laser-wakefield accelerator driven by near-single-cycle pulses. This is an important input for Task 6.2. In addition, simulations indicate that the use of circular laser polarization should reduce the influence of the CEP and thus improve the accelerator stability. The development of such a laser is a challenge that could be discussed in T6.2. At high energy, we have developed a target that had made it possible, for the first time, to combine laser guiding and controlled injection, and thus to produce electron beams with a peaked spectrum at energies above the GeV level. This opens new perspectives for the production of high-quality bemas in the multi-GeV range. The main phenomena that currently limit the quality of the accelerator are the pointing and wavefront instabilities of the laser that induce strong shot-to-shot variations in the charge and peak energy of the electron beams. The reduction of these laser instabilities is the main objective of T6.4

5 References

JOURNAL ARTICLES:

[1] Tomkus V. , Girdauskas V. , Dudutis J. , Gečys P. , Stankevič V. , Račiukaitis G. (2018) High-density gas capillary nozzles manufactured by hybrid 3D laser machining technique from fused silica, *Opt. Express.* 26, 27965

[2] Leemans, W. P. et al. (2006) GeV electron beams from a centimetre-scale accelerator, *Nature Physics* 2, 696-699

[3] Smartsev, S. et al. (2019) Axiparabola: a long-focal-depth, high-resolution mirror for broadband high-intensity lasers. Optics Letters 44, 3414-3417

[4] Rovige L., Huijts J., Vernier A. , Andriyash I., Sylla F., Tomkus V., Girdauskas V., Raciukaitis G., Dudutis J., Stankevic V., Gecys P., and Faure J. (2021) Symmetric and asymmetric shocked gas jets for laser-plasma experiments, *Review of Scientific Instruments* 92, 083302

[5] Rovige L., Huijts J., Andriyash I. A., Vernier A., Tomkus V., Girdauskas V., Raciukaitis G., Dudutis J., Stankevic V., Gecys P., Ouille M., Cheng Z., Lopez-Martens R., and Faure J. (2020) Demonstration of stable long-term operation of a kilohertz laser-plasma accelerator, *Phys. Rev. Accel. Beams* 23, 093401

[6] Julius Huijts J., Igor A Andriyash I. A., Lucas Rovige L., Vernier A., and Faure J. (2021) Identifying obser[7]vable carrier-envelope phase effects in laser wakefield acceleration with near-single-cycle pulses. *Physics of Plasmas* 28.4, 043101

[7] Huijts J., Rovige L., Andriyash I., Vernier A., Ouillé M., Kaur J., Cheng Z., Lopez-Martens R., and Faure J. (2022) Waveform Control of Relativistic Electron Dynamics in Laser-Plasma Acceleration, *Phys. Rev. X* 12, 011036

[8] Gonsalves A. J., *et al.* (2019) Petawatt Laser Guiding and Electron Beam Acceleration to 8 GeV in a Laser-Heated Capillary Discharge Waveguide. *Phys. Rev. Lett.* 122, 084801 (2019)

[9] Oubrerie K., Andriyash I., Lahaye R., Smartsev S., Malka V., and Thaury C. (2022) Axiparabola: a new tool for high-intensity optics, *J. Opt*. 24, 045503

[10] Schmid, K. et al. (2010) Density-transition based electron injector for laser driven Wakefield accelerators, *Physical Review Accelerators and Beams* 13, 091301

[11] Oubrerie K., Leblanc A., Kononenko O. Lahaye R., Andriyash I., Gautier J., Goddet J.-Ph., Martelli L.,Tafzi A., Ta Phuoc K., Smartsev S., and Thaury C. (2022) Controlled acceleration of GeV electron beams in an all-optical plasma waveguide, *Light: Science & Applications* 11, 180

Annex: Glossary

Acronym	Definition
LPA	Laser Plasma Accelerator
CEP	Carrier Envelop Phase
FLICE	Femtosecond Laser Irradiation and Chemical Etching
RMS	Root Mean Square